

CrossMark  
click for updatesCite this: *Chem. Sci.*, 2014, 5, 4184

# Twisting and piezochromism of phenylene-ethynylenes with aromatic interactions between side chains and main chains†

R. H. Pawle,<sup>a</sup> T. E. Haas,<sup>a</sup> P. Müller<sup>b</sup> and S. W. Thomas III<sup>\*a</sup>

This paper describes a series of three-ring phenylene-ethynylenes (PEs) in which specific, non-covalent arene–arene interactions control conformation in the solid-state. As determined by single crystal X-ray structures, edge-face interactions between benzyl ester side chains and conjugated main chains are observed. In contrast, perfluorobenzyl ester side chains interact cofacially with main chains, resulting in ~60° torsional angles between neighboring aryl rings in crystalline PEs. Absorbance and fluorescence spectra of films of these compounds reflect these conformational effects, with the spectra of perfluorobenzyl-substituted compounds shifting hypsochromically from solution- to solid-state. In a demonstration of how balancing non-covalent interactions can open the way to new responsive materials, a main chain twisted derivative with octyloxy substituents displayed significant piezochromic behavior.

Received 19th May 2014

Accepted 5th July 2014

DOI: 10.1039/c4sc01466a

www.rsc.org/chemicalscience

## Introduction

Conjugated organic materials combine semiconducting behavior with the processability, tunability, and flexibility of organics. These features render them useful for applications that require flexible electronics, including display technologies, light sources, sensors, solar cells, and field effect transistors.<sup>1–4</sup> Bandgap engineering of these materials through molecular architecture and geometry has been extensively studied.<sup>5–8</sup> Although the majority of applications require the conjugated material to be in the solid-state, control over solid-state morphology and properties remains an elusive goal critical for optimal performance and fundamental research.<sup>9,10</sup>

Molecules and materials with phenylene-ethynylene (PEs) linkages are an important class of conjugated materials, with applications such as emissive devices and sensors.<sup>11</sup> The coplanarity of aryl rings along the main chain determines effective conjugation and resultant properties such as band gap,<sup>12</sup> while the low rotational barriers about the arylene–alkyne bonds (<1 kcal mol<sup>-1</sup>) generally result in a large distribution of conformers in solution at room temperature.<sup>13</sup> There have been several reported approaches to capture both coplanar (using hydrogen-bonding between monomeric units)<sup>14,15</sup> and twisted

conformations (using steric hindrance along the main chain) of PEs.<sup>16</sup> Large, sterically hindering groups, either as side chains or as part of the main chain, can prevent the extensive  $\pi$ -orbital overlap which is often cited as the cause of reduced and irreproducible luminescence from these materials in the solid-state.<sup>17</sup> Other approaches to preparing twisted PE derivatives include incorporating tethers between aromatic rings,<sup>18,19</sup> binding to a helical template,<sup>20</sup> and the inclusion of positively charged rings.<sup>21</sup>

Side chains are key structural elements of most conjugated materials. In most cases, the nature of side chains do not influence the optoelectronic properties of main chains directly, but can have important implications in solid-state morphology, which makes them useful in tailoring molecular packing for specific applications.<sup>22–26</sup> Despite the ubiquity of aromatic rings in the main chains of conjugated materials, investigations of the potential influence of non-covalent interactions between aromatic rings on side chains and conjugated main chains are uncommon. Interactions such edge-face and cofacial interactions are useful in crystal engineering<sup>27–30</sup> and arranging reactants to undergo processes such as topochemical reactions.<sup>31–33</sup> Herein we report the effects of aromatic interactions between side chains and main chains on the solid-state conformations and optical properties of a series of three-ring PEs.

## Results and discussion

### Solution and solid state optical properties

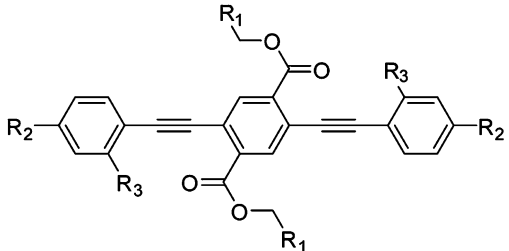
Table 1 shows the structures of a series of seven three-ring phenylene-ethynylenes (1–7) that comprise a central terephthalate ring and terminal phenylacetylene groups. Full

<sup>a</sup>Department of Chemistry, Tufts University, 62 Talbot Avenue, Medford, MA 02155, USA. E-mail: sam.thomas@tufts.edu

<sup>b</sup>Department of Chemistry, Massachusetts Institute of Technology, Cambridge, MA 02139, USA

† Electronic supplementary information (ESI) available: Synthetic procedures, NMR spectra, DSC of 7. CCDC 1003637–1003642. For ESI and crystallographic data in CIF or other electronic format see DOI: 10.1039/c4sc01466a

Table 1 Structures of 1–7



	$R_1$	$R_2$	$R_3$
1	Cyclohexyl	OCH <sub>3</sub>	H
2	Ph	OCH <sub>3</sub>	H
3	F <sub>5</sub> Ph	H	OH
4	F <sub>5</sub> Ph	OCH <sub>3</sub>	H
5	F <sub>5</sub> Ph	H	OCH <sub>3</sub>
6	F <sub>5</sub> Ph	H	H
7	F <sub>5</sub> Ph	OC <sub>8</sub> H <sub>17</sub>	H

syntheses and procedures are available in the ESI.† We chose cyclohexylmethyl (1), benzyl (2), and pentafluorobenzyl (3–7) as the three types of substituents on the central terephthalate ring because of the trend of their quadrupole moments: while cyclohexane has a negligible quadrupole moment, benzene and perfluorobenzene have quadrupole moments that are of opposite sign but similar magnitude.<sup>34</sup> Quadrupole moments of aromatic rings are key to understanding their non-covalent interactions, including edge-face C–H/ $\pi$  and cofacial arene-perfluoroarene interactions. Table 2 summarizes the optical properties of 1–7 in solution and as thin films. We fabricated the films by drop-casting solutions of 3–6 in chlorobenzene onto quartz slides. Although all films we prepared showed scattering due to crystallization of the samples, films of 1 and 2 prepared by drop-casting were too highly scattering for UV/vis spectrophotometry. We obtained films of 1 by spin-casting from CHCl<sub>3</sub>, while we prepared films of 2 by melting a thin layer of powder onto quartz followed by slow cooling.

Table 2 Optical properties of 1–7. All wavelengths are in nm

	Dilute solution <sup>a</sup>			Films	
	$\lambda_{\max, \text{abs}}^b$	$\lambda_{\max, \text{em}}$	$\Phi_F$	$\lambda_{\max, \text{abs}}^b$	$\lambda_{\max, \text{em}}$
1	375	450	0.35	420	481
2	381	461	0.44	392	511
3 <sup>a</sup>	404	461	0.04	405	506
4	383	469	0.49	353	446
5	375	452	0.44	356	443
6	362	425	0.49	342	444
7	386	473	0.46	355, 402 <sup>c</sup>	438, 483 <sup>c</sup>

<sup>a</sup> Measured in CH<sub>2</sub>Cl<sub>2</sub>, except for the fluorescence emission spectrum of 3 (THF), which had  $\Phi_F < 0.01$  in CH<sub>2</sub>Cl<sub>2</sub>, using quinine sulfate in 0.5 M H<sub>2</sub>SO<sub>4</sub> as standard. <sup>b</sup> All maxima represent the lowest energy absorption band. <sup>c</sup> Different maximum upon grinding; discussed at the end of the text.

As depicted in Fig. 1 and the ESI,† 1–3 exhibit bathochromic shifts of absorbance spectra, excitation spectra, or both upon transition from CH<sub>2</sub>Cl<sub>2</sub> solution to the solid-state as thin films. This behavior is typical of PE materials in the solid state and is reported to arise from both planarization of the backbone and intermolecular  $\pi$ -orbital overlap.<sup>23,35</sup> In strong contrast to this behavior, compounds 4–6, all of which have pentafluorobenzyl ester side chains and also lack any phenol groups on the main chain, exhibit hypsochromic shifts upon transition from CH<sub>2</sub>Cl<sub>2</sub>, with decreases in wavelengths of maximum absorbance between 20–30 nm. Observations with the naked eye of powders obtained by simple rotary evaporation of solutions of these compounds corroborate these results; powders of 1–3 are yellow in color, while those of 4–6 are colorless. A recent example of solid-state hypsochromic shift in a three-ring phenylene-ethynylene required highly specific processing conditions to trap the twisted conformation;<sup>36</sup> bathochromic shifts are far more common under general processing conditions used here.<sup>37</sup> Spun cast films of 4–6 initially showed spectra similar to those observed in solution, which we attribute to a broad distribution of conformations due to rapid solvent evaporation.

### X-Ray crystallography

The crystal structures of 1–6 show that specific non-covalent interactions can dictate coplanarity along the PE backbone (Fig. 2 and ESI†). In all structures, the ester groups are highly

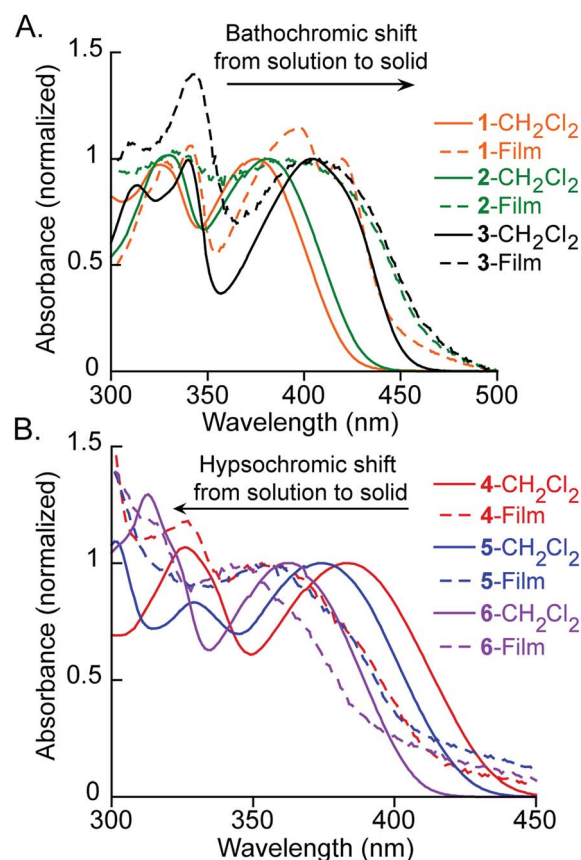


Fig. 1 Absorbance spectra of 1–3 (A) and 4–6 (B) in solution and as thin films.

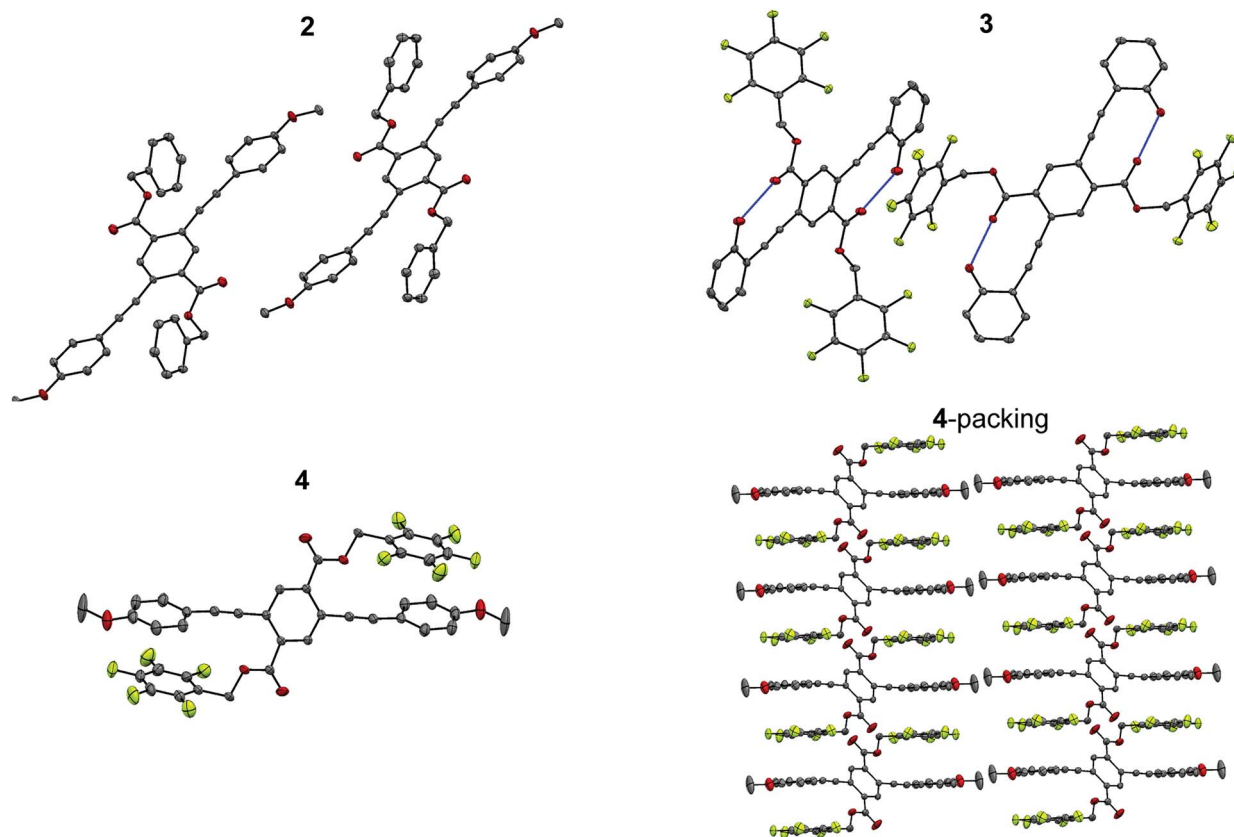


Fig. 2 X-Ray crystal structures of 2–4, (H-bonds in 3 represented by blue lines) and arene–perfluoroarene stacking in 4. Hydrogen atoms omitted for clarity. Thermal ellipsoids shown at 50% probability.

coplanar with the central phenylene ring to maximize  $\pi$ -conjugation of the terephthalate moiety. This structural feature limits the volume of space that the phenyl, perfluorophenyl, or cyclohexyl rings can occupy from the highly coplanar conformation. The cyclohexylmethyl side chains of **1** segregate into aliphatic regions showing no appreciable interactions with the PE main chains. Compound **1** has torsional angles of 17–19° between the central and terminal phenylene rings. Compound **2** shows greater coplanarity of adjacent phenylene rings (torsional angles of 10–14°), which we attribute in part to C–H/ $\pi$  interactions (H-to-centroid distances between 2.62–2.67 Å) between the faces of benzyl substituents of the side chains and hydrogen atoms on the terminal anisyl rings.<sup>38</sup> Compound **3**, which has both perfluorobenzyl esters and phenols on the terminal rings in positions adjacent to the alkyne substituents, shows the greatest coplanarity of all compounds studied in this work, with torsional angles of 1–6°. We attribute this result to hydrogen bonds (O···O distance of 2.79–2.87 Å) between the phenols and the carbonyl oxygen atoms on the central ring, analogous to that observed in solution by Zhao and coworkers.<sup>14,15</sup> Cofacial interactions between main chains, common in crystal structures of PE materials, are not significant in the crystal structure of **3**.

Relative to the central terephthalate ring, the benzyl side chains of **2** and the pentafluorobenzyl side chains of **4–6** occupy a similar volume of space in their interactions with the main chain because the planar ester groups restrict the space

accessible by the side chain. The key side chain–main chain interactions in **4–6**, however, are cofacial interactions between the pentafluorobenzyl side chains and the terminal conjugated rings (ArH–ArF interactions). An inversion of the quadrupole of most perfluorinated benzene derivatives is an important contributor to this well-documented class of cofacial arene–arene interactions. ArH–ArF interactions between main chains are known to exist in conjugated materials, including PEs.<sup>27,30,39</sup> Both intra- and intermolecular ArH–ArF interactions extend throughout the crystal, with centroid to mean-plane distances between cofacially stacked rings of 3.41–3.51 Å. To participate in cofacial interactions with the side chain pentafluorophenyl rings, the terminal rings of the conjugated main chains of **4**, **5** and **6** twist out of coplanarity with the central terephthalate ring, with inter-ring torsional angles of 54–61°. These large deviations from coplanarity reduce the effective conjugation between rings in the structure, and explain why **4–6** show hypsochromically-shifted spectra in the solid-state relative to both dilute solution and solid-state **1–3**. The distributions of conformations of these molecules in solution do not appear to show the same dependence on the non-covalent interactions between side chains and main chains of these compounds as crystalline solids. Evidence for this conclusion are the absorbance spectra of **2** and **4**, which have the same formally conjugated backbone structure, and which differ only slightly in solution but by  $\sim 40$  nm in the solid state.

In addition, the comparison of 3 to 4–6 is a clear demonstration of the competition between different non-covalent interactions: in this case, as has been generally observed in competition between H-bonding and ArH–ArF interactions,<sup>40</sup> the hydrogen bonds dictate the main chain geometry, both forcing the side chain pentafluorobenzyl groups to engage in other intermolecular interactions and yielding the most red-shifted absorbance and fluorescence spectra. To further support our conclusion that changes in torsional angles observed in the crystal structures cause the large differences in solid-state absorbance spectra of 1–3 in comparison to 4–6, we performed TDDFT calculations at the B3LYP/6-31 G(d) level of theory for 2, 3, and 4. We used the same molecular geometry for each TDDFT calculation as that determined from each crystal structure, such that the results of the calculations gave transition energies and oscillator strengths for an individual molecule in vacuum with geometries identical to those found in the single crystals. The trends in energies of the  $S_0$ – $S_1$  transitions from these calculations are consistent with our conclusion relating increased torsional angle in the X-ray structure to hypsochromic shifts in solid-state optical spectra: the calculated transition energies increase from 3 (2.70 eV, 459 nm,  $f = 0.50$ ) to 2 (2.86 eV, 434 nm,  $f = 0.83$ ) to 4 (3.05 eV, 406 nm,  $f = 0.37$ ).

### Piezochromism

Compound 7, which has the same conjugated backbone as 4, but has *para*-octyloxy groups instead of *para*-methoxy groups, has optical spectra in  $\text{CH}_2\text{Cl}_2$  solution that are almost identical to those of 4. In a demonstration of the influence of subtly balanced non-covalent interactions controlling solid-state morphology, solid films of 7 drop-cast from  $\text{CH}_2\text{Cl}_2$  are piezochromic (Fig. 3).<sup>41,42</sup> As initially prepared drop-cast films, the absorbance and fluorescence emission spectra of 7 are red-shifted from corresponding spectra in solution and show green emission ( $\lambda_{\text{max,em}} = 483 \text{ nm}$ ). After heating at 110 °C for 15 minutes, these spectra shift to the blue by 45–50 nm (Table 2 and Fig. 3). Grinding the heated films with a spatula results in complete recovery of green emission, while subsequent reheating (<10 minutes at 110 °C) reverts the film to the blue-emissive phase. In contrast, the optical properties of compounds 1–3 and 6 are unresponsive to pressure. Compounds 4 and 5 respond to pressure with broadened, bathochromically shifted absorbance spectra, but with no new peaks.

While well known in other luminescent materials, to our knowledge, only two PE-based materials are reported to be piezochromic.<sup>43,44</sup> Differential scanning calorimetry (ESI<sup>†</sup>) of 7 after grinding reveals a  $17.5 \text{ J g}^{-1}$  endothermic transition unique to the first heating cycle at 80 °C, above which the sample transitions to the blue-emitting phase. We preliminarily conclude that the twisted main chains adopt a more dense, coplanar conformation upon grinding (the crystal of 3 is  $0.01 \text{ g cm}^{-3}$  more dense than that of 5) that reverts to a twisted conformation coupled with thermally-induced side

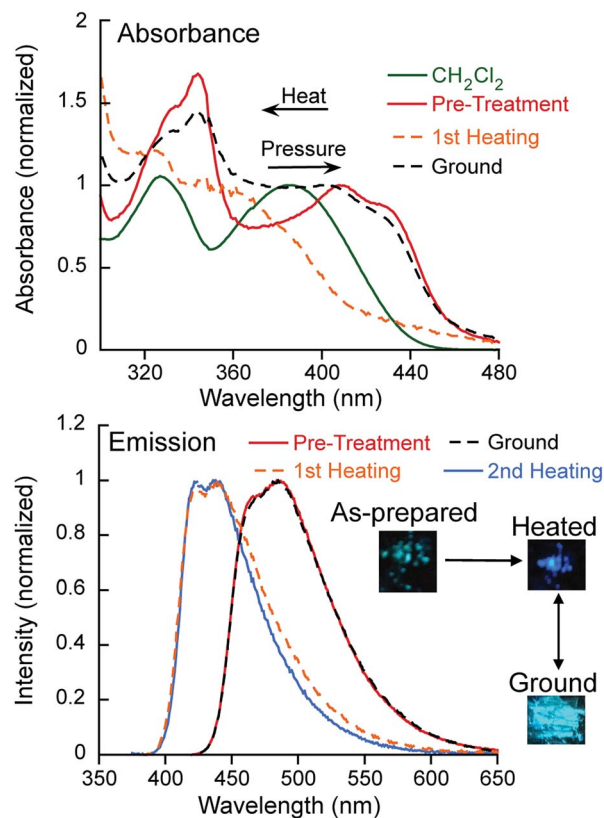


Fig. 3 Absorbance (top) and emission (bottom) spectra of 7, drop cast from  $\text{CH}_2\text{Cl}_2$  with heating and grinding cycles. Excitation wavelengths were 395 nm (green phase) and 350 nm (blue phase).

chain disorder.<sup>45</sup> Although the precise role of the octyloxy chains is not yet clear, we hypothesize that a balance between aliphatic interactions and arene–arene interactions, enabled by the long alkyl chains, are important to the mechanically-responsive phase behavior of 7, and note that strong dependences of alkyl chain length on piezochromic behaviour has been reported in a number of instances.<sup>46–50</sup> Attempts to grow crystals of compound 7 suitable for X-ray crystallography are ongoing.

## Conclusions

In conclusion, we have demonstrated that specific, non-covalent interactions between aromatic rings on side chains and main chains can dictate optoelectronic properties of conjugated materials, and that competition between these and other forces has potential for the design of responsive materials such as piezochromics, particularly in PE materials because of their small rotation barriers. Given the prevalence of aromatic rings in conjugated materials, we believe that specifically designed interactions between aromatic moieties on side chains and main chains represent a rich new approach to side chain engineering and an opportunity for new properties and functionality of these and related systems.



## Acknowledgements

This work was supported by the donors of the American Chemical Society Petroleum Research Fund and 3M through a Non-Tenured Faculty Award. X-ray diffraction instrumentation was purchased with the help of funding from the NSF (CHE-1229426 and CHE-0946721). We also thank Taryn Palluccio for assistance with crystallography.

## Notes and references

- 1 S. R. Forrest, *Nature*, 2004, **428**, 911–918.
- 2 S. W. Thomas, G. D. Joly and T. M. Swager, *Chem. Rev.*, 2007, **107**, 1339–1386.
- 3 T. Muthusamy and J. Sung-Ho, in *Organic Electronics*, CRC Press, 2009, pp. 3–26.
- 4 S. Günes, H. Neugebauer and N. S. Sariciftci, *Chem. Rev.*, 2007, **107**, 1324–1338.
- 5 J. Gierschner, J. Cornil and H. J. Egelhaaf, *Adv. Mater.*, 2007, **19**, 173–191.
- 6 J. Roncali, *Chem. Rev.*, 1997, **97**, 173–206.
- 7 J. Roncali, *Macromol. Rapid Commun.*, 2007, **28**, 1761–1775.
- 8 U. H. F. Bunz, J. N. Wilson and C. Bangcuyo, in *Chromogenic Phenomena in Polymers*, American Chemical Society, 2004, vol. 888, pp. 147–160.
- 9 J. E. Anthony, M. Heeney and B. S. Ong, *MRS Bull.*, 2008, **33**, 698–705.
- 10 Z. B. Henson, K. Mullen and G. C. Bazan, *Nat. Chem.*, 2012, **4**, 699–704.
- 11 U. H. F. Bunz, *Chem. Rev.*, 2000, **100**, 1605–1644.
- 12 M. Hughs, M. Jimenez, S. Khan and M. A. Garcia-Garibay, *J. Org. Chem.*, 2013, **78**, 5293–5302.
- 13 M. Levitus, K. Schmieder, H. Ricks, K. D. Shimizu, U. H. F. Bunz and M. A. Garcia-Garibay, *J. Am. Chem. Soc.*, 2001, **123**, 4259–4265.
- 14 W. Hu, Q. Yan and D. Zhao, *Chem.–Eur. J.*, 2011, **17**, 7087–7094.
- 15 W. Hu, N. Zhu, W. Tang and D. Zhao, *Org. Lett.*, 2008, **10**, 2669–2672.
- 16 J.-S. Yang, J.-L. Yan, C.-K. Lin, C.-Y. Chen, Z.-Y. Xie and C.-H. Chen, *Angew. Chem., Int. Ed.*, 2009, **48**, 9936–9939.
- 17 J.-S. Yang and T. M. Swager, *J. Am. Chem. Soc.*, 1998, **120**, 5321–5322.
- 18 G. T. Crisp and T. P. Bubner, *Tetrahedron*, 1997, **53**, 11881–11898.
- 19 S. Menning, M. Krämer, B. A. Coombs, F. Rominger, A. Beeby, A. Dreuw and U. H. F. Bunz, *J. Am. Chem. Soc.*, 2013, **135**, 2160–2163.
- 20 H. Nakayama and S. Kimura, *J. Phys. Chem. A*, 2011, **115**, 8960–8968.
- 21 T. Terashima, T. Nakashima and T. Kawai, *Org. Lett.*, 2007, **9**, 4195–4198.
- 22 U. H. F. Bunz, J. M. Imhof, R. K. Bly, C. G. Bangcuyo, L. Rozanski and D. A. Vanden Bout, *Macromolecules*, 2005, **38**, 5892–5896.
- 23 U. H. F. Bunz, V. Enkelmann, L. Kloppenburg, D. Jones, K. D. Shimizu, J. B. Claridge, H.-C. zur Loye and G. Lieser, *Chem. Mater.*, 1999, **11**, 1416–1424.
- 24 K. B. Woody, R. Nambiar, G. L. Brizius and D. M. Collard, *Macromolecules*, 2009, **42**, 8102–8111.
- 25 P. Samorì, V. Francke, V. Enkelmann, K. Müllen and J. P. Rabe, *Chem. Mater.*, 2003, **15**, 1032–1039.
- 26 J. Mei and Z. Bao, *Chem. Mater.*, 2014, **26**, 604–615.
- 27 C. Dai, P. Nguyen, T. B. Marder, A. J. Scott, W. Clegg and C. Viney, *Chem. Commun.*, 1999, 2493–2494.
- 28 C. Mallet, M. Allain, P. Leriche and P. Frère, *CrystEngComm*, 2011, **13**, 5833.
- 29 M. Nishio, *CrystEngComm*, 2004, **6**, 130.
- 30 F. Ponzini, R. Zagha, K. Hardcastle and J. S. Siegel, *Angew. Chem., Int. Ed.*, 2000, **39**, 2323–2325.
- 31 G. W. Coates, A. R. Dunn, L. M. Henling, J. W. Ziller, E. B. Lobkovsky and R. H. Grubbs, *J. Am. Chem. Soc.*, 1998, **120**, 3641–3649.
- 32 S. K. Collins, Y. El-Azizi and A. R. Schmitzer, *J. Org. Chem.*, 2007, **72**, 6397–6408.
- 33 Y. El-azizi, A. Schmitzer and S. K. Collins, *Angew. Chem., Int. Ed.*, 2006, **45**, 968–973.
- 34 E. V. Anslyn and D. A. Dougherty, *Modern Physical Organic Chemistry*, University Science Books, Sausalito, CA, 2006.
- 35 J. Kim and T. M. Swager, *Nature*, 2001, **411**, 1030.
- 36 R. Gupta, R. Thomas and G. U. Kulkarni, *J. Mater. Chem.*, 2012, **22**, 19139.
- 37 Y. Yamaguchi, Y. Shimoi, T. Ochi, T. Wakamiya, Y. Matsubara and Z. Yoshida, *J. Phys. Chem. A*, 2008, **112**, 5074–5084.
- 38 W. B. Jennings, B. M. Farrell and J. F. Malone, *Acc. Chem. Res.*, 2001, **34**, 885–894.
- 39 S. S. Babu, V. K. Praveen, S. Prasanthkumar and A. Ajayaghosh, *Chemistry*, 2008, **14**, 9577–9584.
- 40 R. Berger, G. Resnati, P. Metrangolo, E. Weber and J. Hulliger, *Chem. Soc. Rev.*, 2011, **40**, 3496–3508.
- 41 Y. Sagara and T. Kato, *Nat. Chem.*, 2009, **1**, 605–610.
- 42 Z. Chi, X. Zhang, B. Xu, X. Zhou, C. Ma, Y. Zhang, S. Liu and J. Xu, *Chem. Soc. Rev.*, 2012, **41**, 3878–3896.
- 43 Y. Sagara and T. Kato, *Angew. Chem., Int. Ed.*, 2008, **47**, 5175–5178.
- 44 Y. Sagara, S. Yamane, T. Mutai, K. Araki and T. Kato, *Adv. Funct. Mater.*, 2009, **19**, 1869–1875.
- 45 M. D. Curtis, J. I. Nanos, H. Moon and W. S. Jahng, *J. Am. Chem. Soc.*, 2007, **129**, 15072–15084.
- 46 J. Kunzelman, M. Kinami, B. R. Crenshaw, J. D. Protasiewicz and C. Weder, *Adv. Mater.*, 2008, **20**, 119.
- 47 J. Kunzelman, B. R. Crenshaw, M. Kinami and C. Weder, *Macromol. Rapid Commun.*, 2006, **27**, 1981–1987.
- 48 W. Liu, Y. L. Wang, L. Y. Bu, J. F. Li, M. X. Sun, D. T. Zhang, M. Zheng, C. Yang, S. F. Xue and W. J. Yang, *J. Lumin.*, 2013, **143**, 50–55.
- 49 N. D. Nguyen, G. Q. Zhang, J. W. Lu, A. E. Sherman and C. L. Fraser, *J. Mater. Chem.*, 2011, **21**, 8409–8415.
- 50 W. Liu, Y. L. Wang, M. X. Sun, D. T. Zhang, M. Zheng and W. J. Yang, *Chem. Commun.*, 2013, **49**, 6042–6044.